ELSEVIER

Polymer 41 (2000) 1917–1935

polymer

Characterization of synthetic membranes by Raman spectroscopy, electron spin resonance, and atomic force microscopy; a review

K.C. Khulbe*, T. Matsuura

Industrial Membrane Research Institute, Faculty of Engineering, Department of Chemical Engineering, University of Ottawa, 161 Louis Pasteur Street, P.O. Box 450, Stn. A, Ottawa, ON, Canada KiN 6N5

Received 15 February 1999; received in revised form 10 May 1999; accepted 18 May 1999

Abstract

In this article an attempt is made to review critically the papers concerning novel membrane characterization methods. In particular, our focus on Raman spectroscopy, electron spin resonance (ESR) and atomic force microscopy. For each method the general principle is briefly outlined, followed by discussions on characterization of polymeric materials, in general, and synthetic polymeric membranes, in particular. After highlighting several examples, discussions are made on advantages for each method in order to identify specific area of applications. In general, Raman Spectroscopy is most adequate to obtain information on crystalline structure of the macromolecules and, change of polymeric structure in membrane, ESR on the mobility of molecules in membrane polymer matrixes and membrane pores, and Atomic Force Microscope for three-dimensional display of membrane surfaces.

Keywords: Atomic force microscope; Raman scattering; Electron spin resonance

1. Introduction

The development, for seawater desalination, of asymmetric membranes with a thin selective layer supported by a porous sublayer opened up a new avenue in membrane separation technology during the nineteen sixties [1]. Over the past 35 years membrane separation technology has grown into an annual one billion-dollar industry worldwide. There are a number of membrane separation processes currently being used. Typical examples are: reverse osmosis (RO), ultrafiltration (UF), microfiltration (MF), pervaporation, and membrane gas and vapor separation.

It is generally accepted that the control of the polymer morphology in the selective skin layer is very crucial for the design of a synthetic polymeric membrane. Many attempts have been made therefore during the past 35 years to establish the cause and effect relationship between membrane preparation, polymer morphology and membrane performance. Although all these attempts were valuable to cast some light on the mechanism of membrane formation and membrane transport, the understanding of the phenomena seems insufficient, mainly due to the complex nature of the mechanism. This work addresses the characterization of the polymeric structure in the synthetic polymeric membrane by using novel characterization techniques.

There are three important structural levels in the polymeric membrane: (i) The molecular, which is equivalent to the chemical nature of the polymer. It is characterized by polar, steric and ionic factors. It is also responsible for the microcrystalline nature. (ii) The microcrystalline, which affects both the transport and the mechanical properties of membrane. (iii) The colloidal, which is concerned with the aggregation of macromolecules and governs the statistics of pores (pore size, pore size distribution, pore density and void volume). It is desirable to develop new characterization methods at each level to achieve more rigorous understanding of the polymeric structure in the membrane. The objective of this paper is, therefore, to propose some novel characterization methods and to review the results that have been so far obtained by applying these novel methods.

Different approaches can be used to characterize the membranes, which can be classified according to structure and permeation related parameters. There are various well-established methods for characterizing the membrane, which are as follows:

1. Microscopic.
2. Bubble gas transport method.
3. Mercury porosimetry.
4. Liquid vapor equilibrium.
5. Gas liquid equilibrium.
6. Liquid solid equilibrium method.

* Corresponding author. Tel.: +1-613-562-5772; fax: +1-613-562-5172.

0032-3861/00/$ - see front matter
PII: S0032-3861(99)00359-6

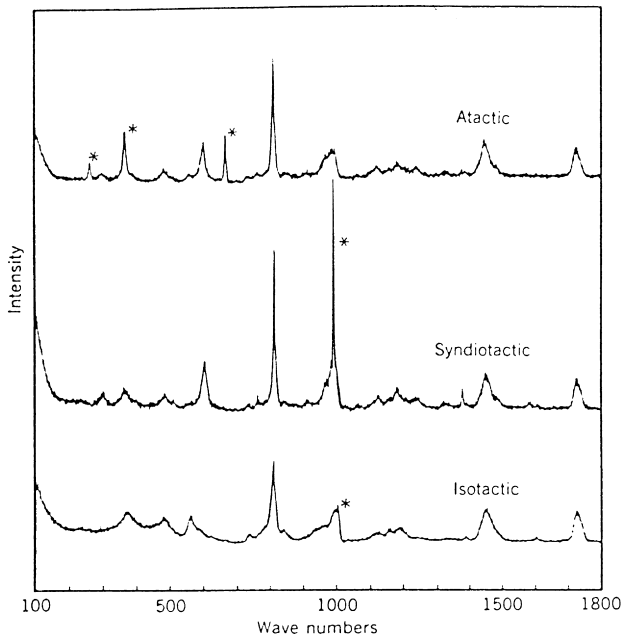

Fig. 1. VV polarized Raman spectra of various tacticities of PMMA. Bands with asterisks indicate residual solvent from the spinning process used to form the films. Sampling was carried out by waveguide RS.

These methods are discussed in the literature [2].

There are newly developed methods for the characterization of membranes, especially for surface morphology. These are as follows;

1. Electron Spin Resonance (ESR).
2. Atomic Force Microscopy (AFM).
3. Raman Spectroscopy (RS).
4. Nuclear Magnetic Resonance (NMR).
5. Neutron Scattering Technique.

In this review only ESR, AFM and RS will be discussed. The latter two are only recently being applied to membrane technology. Unfortunately, not much literature is available on these methods.

2. Raman scattering

2.1. General principle

The infrared and Raman spectra of a molecule compliment each other and information on the complete vibrational spectrum of a molecule often requires both infrared and Raman vibration. For example, the symmetrical stretching, ν_1 (normal vibration) of CO_2 is infrared inactive, but active in Raman. On the contrary, the bending, ν_2, and asymmetric stretching, ν_3, vibrations are Raman inactive. Infrared absorption occurs when the interaction of the molecule with light produces a change in the dipole moment during a normal vibration. RS occurs when the molecular motion produces a change in the polarizability of the molecule. Changes in the stereoregularity bring about changes in the Raman spectra. Raman spectra, in particular, give information about groups like –C–S–, –C–C–, –N=N–, and –C=C– whereas IR can be used to characterize the group like OH, C=O, P=O, and NO_2. Galeski and Pirkowska [3] detected strain defects and holes formed during crystalline growth in isotactic propylene by RS.

In RS, light scattered by the molecules contains frequencies other than that of incident monochromatic light. It is the differences between the frequencies of scattered light and the frequency of the incident light that correspond to the normal vibrational frequencies of the molecules. When a molecule absorbs radiations, its energy increases in proportion to the photon.

$$E = h\nu = hc/\lambda,$$

where c is the velocity of light; h the Planck's constant; λ the wave length of the radiation; and ν the frequency. The increased energy may be at the level of the electronic, vibrational or rotational energy of the molecule. Interaction between molecular units and their surroundings can be readily detected by perturbations in the Raman spectra.

2.2. Application in polymers

The main advantage in polymer characterization RS is in the ease of obtaining a good spectrum with little or no sample handling. This process is extremely valuable in many different cases for polymer characterization. It can be used to determine the functional groups, and group structure, conformation and orientation of the chains and to follow changes in the structural parameters as the polymers are exposed to environmental or mechanical stresses. Hydrogen bonding, crystal field splitting, and chain packing are all examples of modification to the surrounding field of the molecular unit, which can be studied by RS. It is also very sensitive to the thermal history of the polymer. Raman polarization studies can give detailed information about the distribution of orientations of structural units for both crystalline and noncrystalline regions. However, optical clarity and fluorescence can cause trouble, especially with impure and chemically complex samples. Another problem, specific to polarization studies, is the scrambling caused by multiple scattering in a heterogeneous system. Raman polarization measurements on polymers can provide extremely valuable structural information; but they are sometimes difficult to obtain. Studies on molecular conformation of polymers are extremely dependent upon accurate polarization measurements. An important area of research in polymer studies involves how the physical and mechanical properties of a polymer are influenced by molecular orientation induced by drawing. Disordered polymers give vibrational modes that are all active in infrared and RS.

An important area of research in polymer studies involves how the physical and mechanical properties of a polymer are influenced by molecular orientation induced by drawing.

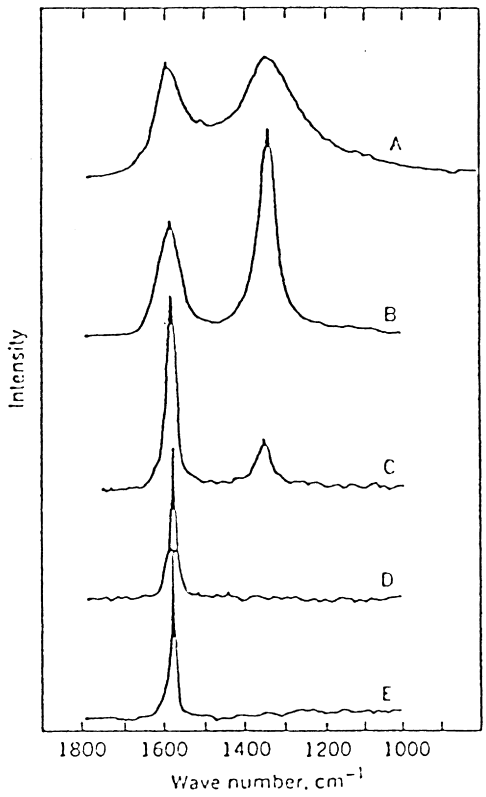

Fig. 2. Raman spectra of oriented poly(*p*-phenylene vinylene) films pyrolyzed at: (a) 950°C; (b) 2000°C; (c) 2500°C; (d) 2750°C; and (e) 3000°C.

Polymers are varied between amorphous and crystalline state. The crystallinity content depends on the molecular weight of the polymer. Low molecular weight polymer will have a high content of crystallites in comparison with high molecular weight polymer. Various morphologies are possible between a completely crystalline and completely amorphous conformation. The formation of a crystalline region depends on the time allowed for the polymer to crystallize from solution. Crystalline polymers have a number of morphological features that can be studied by RS. Local structural effects determined include the amount of remaining amorphous content [4,5] and type of order induced by processing, defects in structure [3] and in some cases tacticity [6]. Fig. 1 shows the effect of tacticity in poly(methyl methacrylate) (PMMA) thin films on Raman spectra. It is evident that polymer can exist in a number of configurations that can be syndiotactic and isotactic or helical and planar. Alternatively, they can be atactic with an ordered conformation [7]. Many phase transitions can be monitored by following the changes in the RS associated with the crystalline structure [8]. A review that contains several examples of the use of RS to clarify polymer structure is given in Ref. [9]. Ko [10] applied RS technique to study polyacrylonitrile (PAN) fibers during graphitization and reported that RS can be correlated to the mechanical properties of the fiber. He observed that the Raman specific absorption peak of noncrystalline carbon layers (1360 cm^{-1}) weakened with the increase in the graphitization temperature, whereas the degree of graphitization rose.

Fig. 2 shows the transformations of poly(*p*-phenylene vinylene) to a graphite structure during pyrolysis [11]. As the temperature increases, the film transforms completely to graphite carbon, as shown by the loss of the 1360 wave number band and narrowing of the 1580 wave number band associated with carbon–carbon double bond.

Koenig et al. [12,13] studied the structure of poly(ethyleneoxide) (PEO) in aqueous solution. Fig. 3 shows the spectra of crystalline PEO and PEO in a 10% water solution. The crystalline is complex, showing several sharp bands with characteristic helical splitting. The melt PEO has broader bands at shifted frequencies and no band splitting is detected. This indicates the helical structure of the solid polymer is lost upon melting. The spectrum of PEO in water looks much more like the crystalline polymer indicating that considerable helical structure is left upon dissolution. Gall et al. [14] studied laser Raman spectrum of several samples of polyethylene and made full assignment of the observed Raman spectrum in terms of fundamental modes, overtones and combinations. Zerbi [15] discussed the molecular vibrations of the perfect as well as highly disordered polymers on the basis of RS. Grasselli et al. [16] discussed the Raman applications in polymers in detail.

Raman spectroscopy has also been applied to some studies of the mechanism of polymer reactions. Koenig [7] observed by RS that polymerization of butadiene can yield many different molecular structural products. The effect of cross-linking on the Raman spectra of epoxy resin has been studied by Lu and Koenig [17]. A similar study has been made by Koenig and Shih [18] on unsaturated polyester resins containing styrene. In the hope of obtaining some sight into the fracture mechanism of polymers, the effect of mechanical stress on the RS spectra of polypropylene, polycarbonate, polystyrene and nylon 6,6 have been examined [19]. Gailliez-Degremont et al. [20] used RS technique to study polyamines adsorbed onto silica gel and reported that polyamine adsorption onto silica occurred with two kinds of polymer population: chemisorbed (interactions between silanol and the nitrogen atom) and physisorbed (multilayer polymers). The modifications of chemisorbed polymer bands were stronger than physisorbed bands.

2.3. Application to polymeric membranes

There are three different Raman spectroscopic methods, which can be used for surface studies: microprobe, internal reflection and surface enhanced Raman spectroscopy (SERS) [21]. Raman methods [22–24] also allow a very small surface area (1 μm^2) to be measured. Analyses of a cross section of a specimen allow this method to be used for depth profiling with a resolution of the order of 1 μm. Structures of the surface can be studied also for laminate polymers [25,26] and embedded materials [27]. RS can be

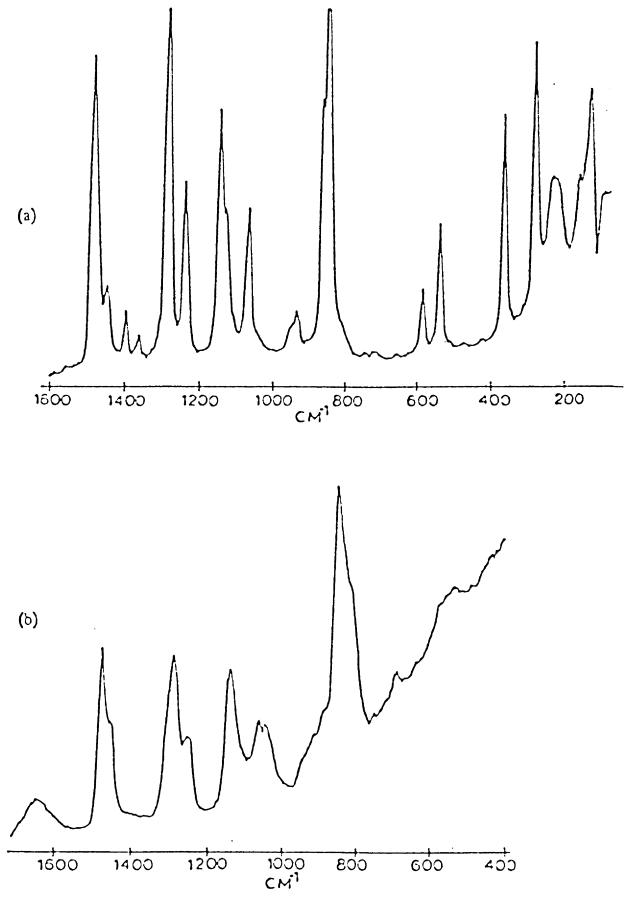

Fig. 3. Raman spectra of polyethylene oxide: (a) solid PEO; (b) 10%

obtained ranging from a few tenths of a nanometer to several micrometers of thickness of polymer coated on a surface [21]. With care, the Raman effect can be measured without disturbing the film or surface.

The Raman effect is sensitive to the molecular environment in many ways as discussed above. The bulk properties of a polymer can be drastically modified by variation in morphology, thus, the knowledge of and controls over the morphology are technologically important. As polymeric films can be processed in a variety of ways (casting of solutions by doctor blade or spinning), it is fairly common that some orientation, either in plane or out of plane, will be induced. When RS is applied to the membrane, the morphology of the membrane, including the orientation of polymer chain and the degree of crystallinity of the polymer in the membrane, can be studied. It also enables monitoring of the morphology change during membrane formation. The morphology-membrane transport relationship will help to reveal the mechanism of mass transport in the membrane. RS may also contribute to establish the transport of permeating molecules, either in gas or liquid form, through the membrane "pore". There has been so far no work to correlate RS and permeation properties of membrane.

Fig. 4 shows the Raman spectra of various form of polyethylene [16,28]. In (a) the RS of a wax lump with molecular weight around 800 is shown. It melts at around 75C. An unoriented film gave the spectrum in (b). Spectra of high density, high melting point forms with a molecular weight 10^4–10^5 are shown in (c) and (d). The intensity of the feature at 890 cm^{-1} is a rough inverse indicator of the

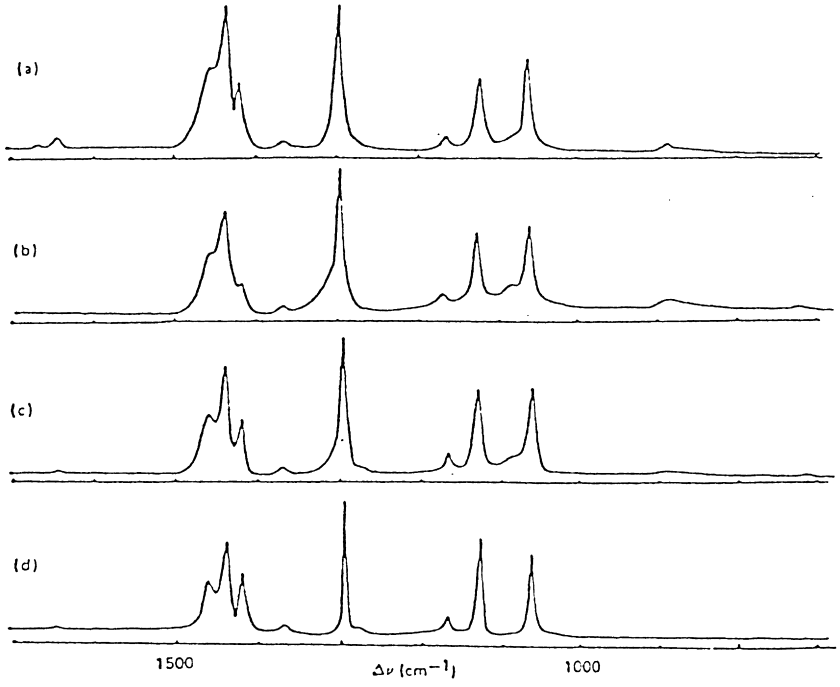

Fig. 4. Raman spectra of polyethylene: (a) wax lump with molecular weight around 800; (b) unoriented film, molecular weight around 10^4; and (c) unoriented film, molecular weight around 10^5.

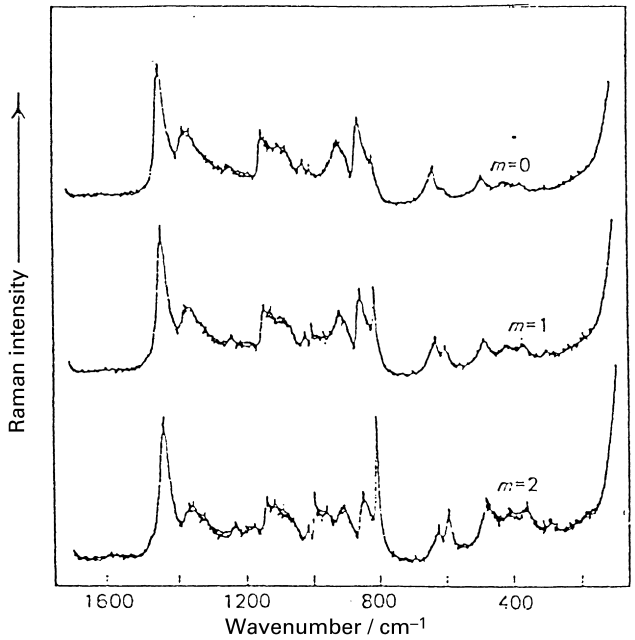

Fig. 5. RS from a PVA/PMMA laminate for the $m = 0, 1$ and 2 modes.

molecular weight. Crystallinity, a desirable characteristic from the standpoint of oxidative degradation, is indicated by the sharpness of the bands at 1300 and 1400–1500 cm^{-1}. Thus (b) with a crystallinity of 50% exhibits the widest Raman lines; (d) with almost total crystallinity (the extended chain form) shows the narrowest lines. When molecular chain terminates in a vinyl grouping, the features around 1650 cm^{-1} appears. Consideration of molecular weight, degree of crystallinity, etc. is important because of the relationship of these factors to physical properties such as hardness, brittleness, permeability, impact resistance, etc.

Chemical modification, such as that occurring during ion implantation in polymers, has also been monitored by Raman spectroscopy [29]. Zubov et al. [30] studied the effect of the solvent and polymeric solid interactions. Films were prepared from polystyrene by using three different solvents, i.e. xylene, chloroform and a mixture of aromatic hydrocarbons. With each solvent, changes were observed in the properties of films such as tensile strength, adhesion and thermo-physical constant. Frazer et al. [31] studied the deformations and cooling effects on the lamellar structure of high-density polyethylene (PE). However, the interpretation of RS of branched polymer is essentially

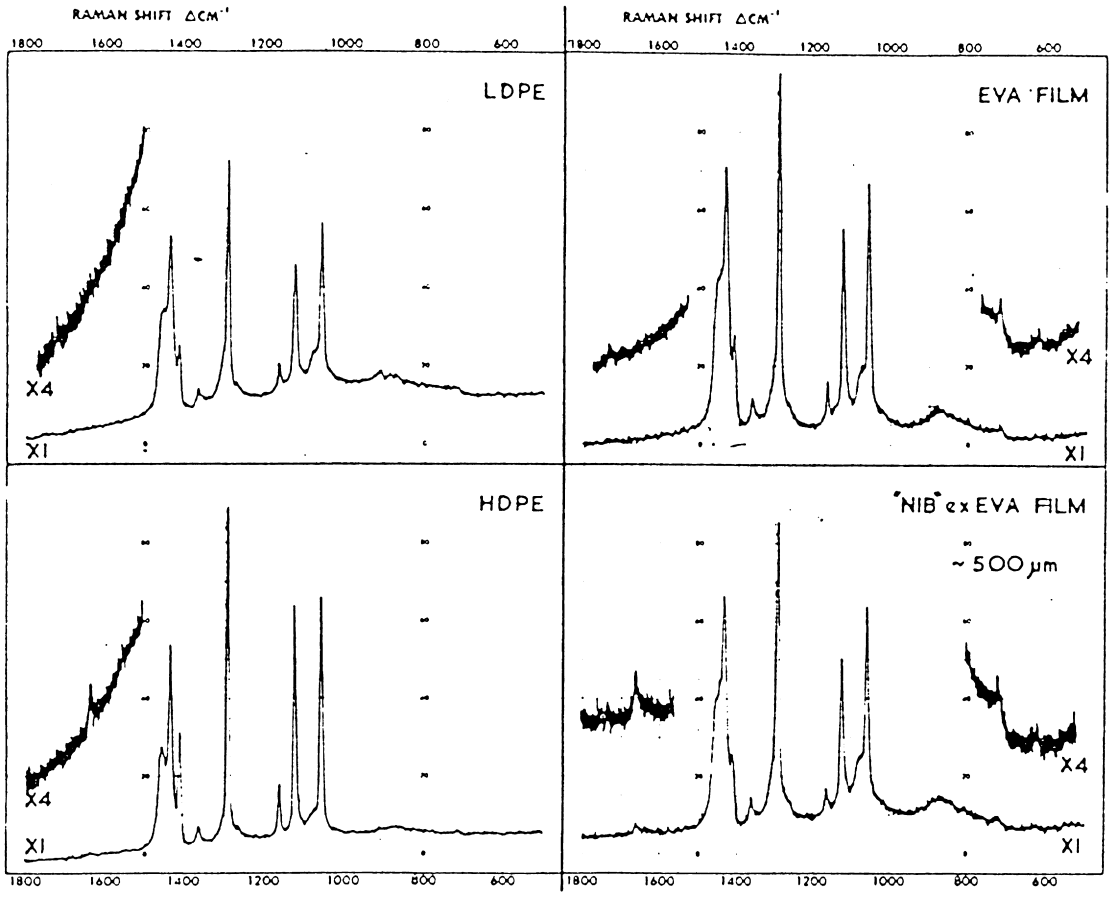

Fig. 6. Raman spectra of impurity from a polymer film and spectra of associated material: (a) low-density PE; (b) high-density PE; (c) ethylene vinyl acetate film; and (d) ethylene vinyl acetate film containing small speck of foreign material suspected to be another polymer, (a) and (b).

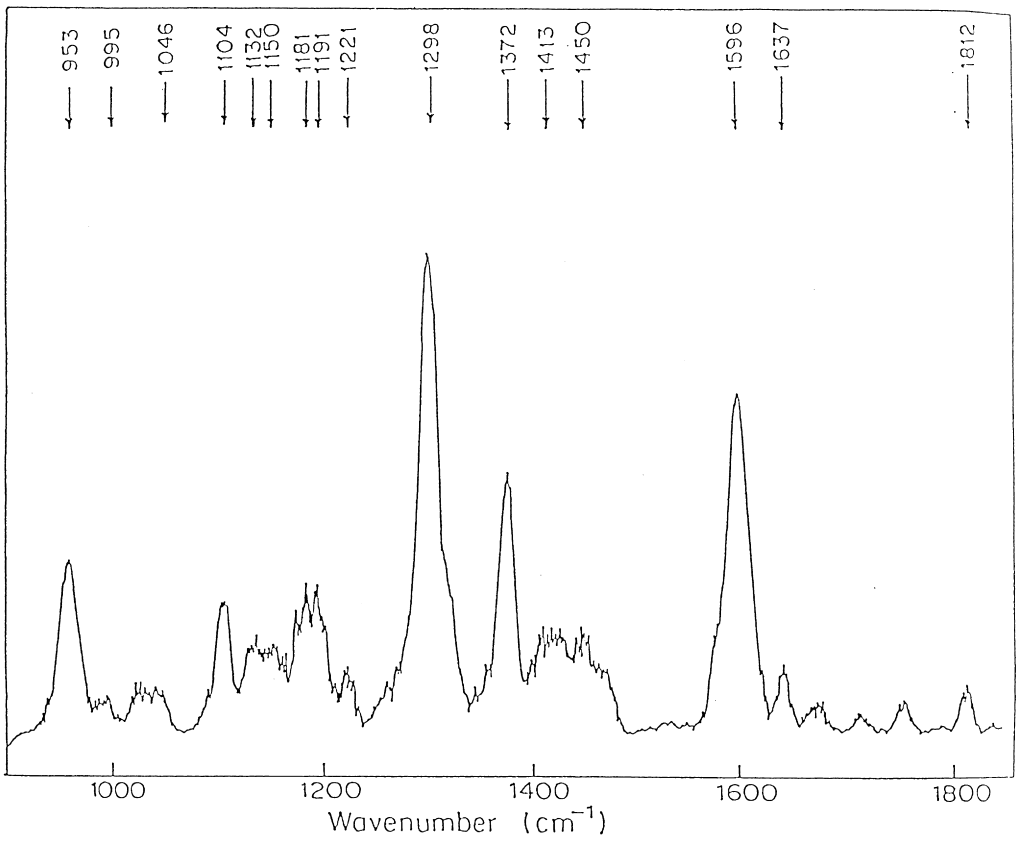

Fig. 7. Raman spectra of PPO-powder.

complex. A benzene ring with a halogen has a total of 30 modes of vibrations.

Schlotter and Rabolt [32], and Rabolt and Swalen [33] described in detail the surface of polymer films by wave-guide Raman spectroscopy (WRS). Fig. 5 shows the WRS of the poly(vinyl alcohol)/poly (methyl methacrylate), (PVA)/(PMMA) laminate for the $m = 0, 1$ and 2 modes (m is the mode of vibration). They interpreted their results such that at the interface of two polymers, the –OH group on the backbone of PVA coupled with a similar concentration of C=O groups in PMMA. It was suggested that WRS might provide a very sensitive probe of interfacial interaction in layered structures of polymers.

RS can be used for examining impurities in polymer films. Fig. 6 shows the RS of ethylene vinyl acetate (EVA) film containing a small speck of foreign material suspected to be another polymer [16,34]. There are also for reference 'pure' EVA film and two suspected impurities, i.e. low- and high-density PE. Although the spectra are generally very similar, small differences can be noted. For example, high-density PE has a band at 1640 cm^{-1} assigned to terminal vinyl $–C{=}CH_2$ groups which does not appear in the low-density PE. The spectrum of the impurity also shows unsaturation, but it occurs at 1660 cm^{-1} and is assigned to *trans* CH=CH This type of unsaturation occurs when EVA polymer is heated and acetic acid evolves. Thus, the impurity appears to be due to thermal decomposition of the polymer and not to be due to either type of PE.

Chemical structure of a membrane is meant to be the combination of steric and polar properties of membranes prepared from polymer at the submacromolecular level. This includes chain segments and functional groups. Khulbe et al. [35,36] studied poly(phenylene oxide) (PPO) powder and dense homogeneous membranes prepared from it by RS (Fig. 7). Table 1 shows the solvents used for the preparation of PPO membranes, boiling point (BP) of solvents and the code name given to the membranes. It was noticed that the '*state-of-polymer*' in the membrane depends on the solvent used for casting membranes. Fig. 8 shows the change in the intensities at various Raman frequencies in the PPO membranes against the boiling point of the solvents used for the preparation of membranes. From Fig. 8, it seems that PPO–CS_2 membrane has minimum intensity (area) at 1298, 1191–1181 and 953 cm^{-1} bands of RS when compared with the areas of other studied membranes. These bands are assigned to $> O <$, plane C–H band and C–H stretches and CH3 rocking, respectively, for PPO RS [31]. It was observed that the selectivity for CO_2/CH_4 and O_2/N_2 gas pairs was the highest for the PPO–CS_2 membrane when compared with the selectivity observed for the above gas pairs for other membranes (Fig. 9). The permeation rate, on the other hand, increased with the increase in the boiling

Table 1
Boiling point (Langes' Handbook of Chemistry, 9th ed., Sandusky, OH: Handbook Publishers, 1956 and Lide DR, editor. CRC handbook of chemistry and physics, 73rd ed. Boca Rotlon, FA, 1992–1993.) of the solvents used for the preparation of the PPO membrane and the name given

Solvent	Boiling point (°C)	Name of the membrane given
Carbon disulfide	46.3	PPO–CS_2
Benzene	80.1	PPO–C_6H_6
Trichloro-ethylene	86.7	PPO–TCE
Toluene	110.6	PPO–$CH_3C_6H_5$
Chlorobenzene	132	PPO–ClC_6H_5
Bromobenzene	156.2	PPO–BrC_6H_5

point of the solvents used (Figs. 10 and 11) with the exception for PPO–CS_2 membrane. It can be concluded, therefore, the structural change revealed by RS is correlated to the membrane performance. The details of the structural change are currently under study.

The future of Raman studies on polymeric membrane appears to hold a great potential for many different applications. Study of the crystalline structure of polymers will add to the existing knowledge of intramolecular forces in crystals and their effect on stable polymer structures. The use of vibrational spectroscopy will help to understand the relationship between structure and transport properties, which could have an important impact on designing membranes for specific separation problems. RS study of isotropic polymeric membranes can be related with the permeability by using free volume as an intermediary property. However, no such work has been carried out so far.

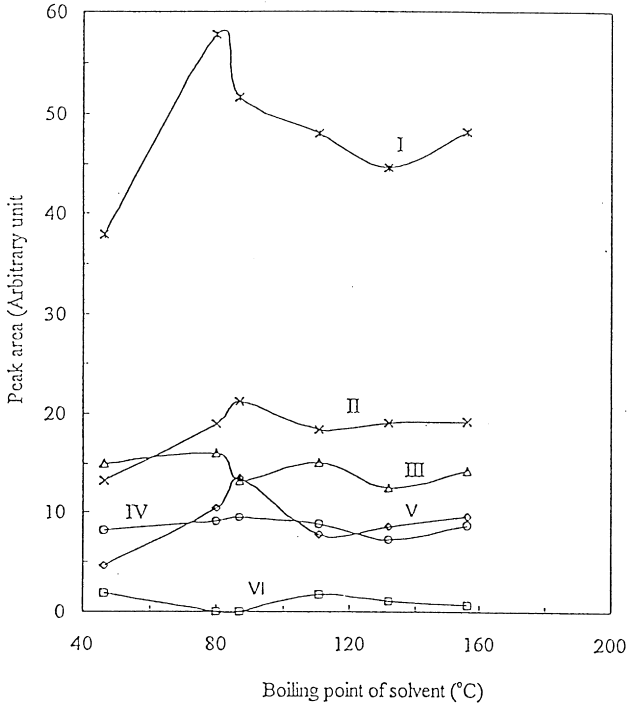

Fig. 8. Peak area (arbitrary) of RS vs. BP of the solvent used for the preparation of membrane. I-★: 1298 cm^{-1}; II-×: 953 cm^{-1}; III-△: 1372 cm^{-1}; IV-○: 1104 cm^{-1}; V-◇: 1191–1181 cm^{-1}; VI-□: 1046–989 cm^{-1} (top surface of the membrane).

3. Electron spin resonance

3.1. General principle

Many books are available on the theory and the application of ESR, which is also known as the electron paramagnetic resonance (EPR). In simple words ESR phenomenon can be defined as follows: 'Paramagnetic molecules have unpaired electrons, and in changing the magnetic field these will absorb energy at particular values of the field. This absorption is due to a change in direction of the magnetic moment resulting from the electron's spin. The absorption spectra that are produced can give information about the structure of free radicals and complex ions that is unobtainable by other methods' [37]. ESR works on the same principle as NMR except that microwave (rather than radio wave) frequencies are employed and spin transitions of unpaired electrons rather than nuclei are recorded. Unlike NMR spectra, where absorption is recorded directly, ESR spectrometers plot the first derivative of the absorption curve.

ESR permits observation of any substance having unpaired electrons. Some examples of substances that exhibit this quality are as follows:

1. Atoms or ions having partially filled inner electron shells that are all of the transition elements of the iron series, rare earth's and platinum series.
2. Molecules having an odd number of electrons in their outer shells (e.g. NO or ClO_2).
3. Molecules with an even number of electrons in their outer shells but with a resultant magnetic moment (e.g. O_2).
4. Free radicals, which are naturally or artificially produced.
5. Conduction electrons in metals and acceptors and donors in semiconductors.
6. Modified crystal structure and defects in crystals e.g. color centers.

ESR study is affected by the degree of detail desired and by the type of problem investigated. It is sensitive to local environment.

It can be seen from quantum mechanics that every electron acts as a magnetic dipole and, as such, if it is placed in a static magnetic field, H, can have only two possible orientations, with or against the field. In thermal equilibrium the greater number of electrons occupy the lower energy levels according to the Boltzmann statistics. In the presence of an electromagnetic variation field electrons in the lower energy levels can absorb photons of energy, $h\nu$ (h is the Planck's constant and ν the frequency) and thereby are excited to a higher energy level which corresponds to the energy absorbed. The absorption energy can be observed as a function

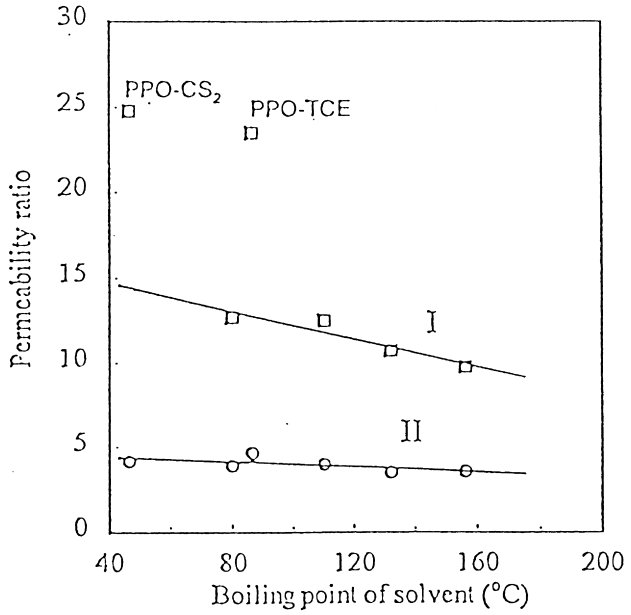

Fig. 9. Permeability ratio of CO_2/CH_4 and O_2/N_2 vs. BP of the solvent used for membrane preparation, I-□, CO_2/CH_4; II-○, O_2/N_2.

of external applied field value by means of high frequency technique. The relation between field value and measuring frequency can be described quantitatively as follows:

$$h\nu = g\beta H,$$

where g is the spectroscopic splitting factor or Lande's constant and β the Bohr constant. The g value of a free electron is 2.0035. The magnetic interactions between the electron spins and nuclear spins cause the ESR spectrum to consist of a number of lines rather than a single line. The arrangement of the resulting group of lines in the ESR spectrum is called the hyperfine structure of the spectrum.

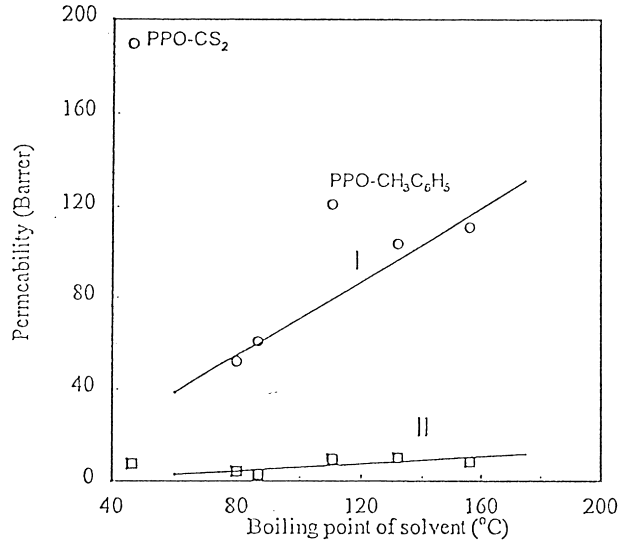

Fig. 10. Permeability of O_2 and N_2 vs. BP of the solvent used for the membrane preparation. I-○: O_2; II-□: N_2.

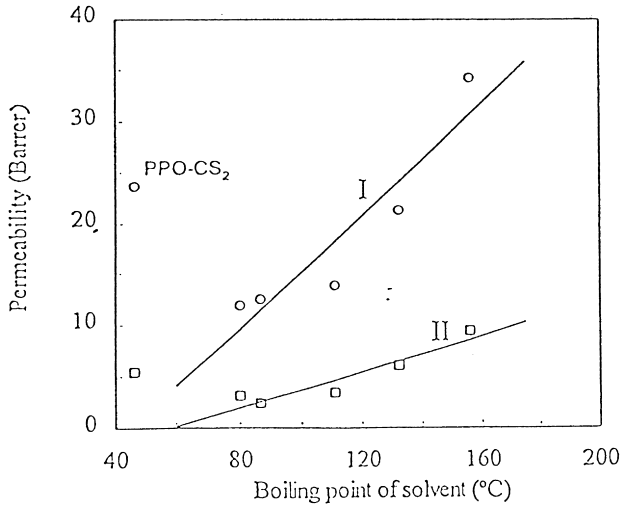

Fig. 11. Permeability of CO_2 and CH_4 vs. BP of the solvent used for the membrane preparation. I-○: CO_2; II-□: CH_4.

3.2. Radicals in polymers and polymeric membranes

Polymers themselves contain paramagnetic free radicals. It is possible that these radicals may take part in the transportation of gases through the membrane. It is observed that these radicals are affected reversibly with gases. Khulbe et al. [38] observed that PPO radicals in PPO-powder and in membranes prepared from it contain free radicals that are affected by the conditions of the environment. Table 2 shows the number of spins/g (concentration) in all studied membranes. It seems that the number of spins/g in membranes is higher than in the PPO-powder and it also depends on the characteristics of solvents. Generally, the number of spins/g in vacuum is less than in presence of air. However, no definite conclusion could be drawn due to small quantity of spins (10^{14} spins/g). It was noticed that in presence of N_2 the number of spins/g (concentration) was more than that in presence of O_2. On the contrary, the number of spins/g (concentration) was higher in presence of CH_4 than CO_2. The permeation rates through the membrane of CO_2 and O_2 are usually higher than CH_4 and N_2, respectively. This type of behavior also was observed with sulfonated and brominated PPO membrane [39]. Oxygen reduces the number of spins either physically or chemically [40]. From Table 2, it seems that PPO–CS_2 and PPO–TCE membranes have a lesser number of spins/g when compared with the number of spins/g (concentration) of other membranes at the similar environment with few exceptions. It was observed that the selectivities of PPO–CS_2 and PPO–TCE membranes for CO_2/CH_4 and O_2/N_2 gas pairs were higher than those for other membranes [35]. Table 3 shows the ratio of number of spins/g in membrane in presence of CO_2 and CH_4, and O_2 and N_2. From Table 3, it seems that there is not much change in the ratio of the paramagnetic radicals for PPO–CS_2 and PPO–TCE membrane when compared with the ratio obtained for

Table 2
Number of spins/g in PPO and the membranes under different environments

In presence of	PPO-powder ($\times 10^{-14}$)	PPO–CS_2 ($\times 10^{-14}$)	PPO–C_6H_5 ($\times 10^{-15}$)	PPO–TCE ($\times 10^{-14}$)	PPO–$CH_3C_6H_5$ ($\times 10^{-15}$)	PPO–ClC_6H_5 ($\times 10^{-14}$)	PPO– BrC_6H_5 ($\times 10^{-14}$)
Vacuum	7.5	12.9	23.8	23.1	16.2	27.3	11.1
Air	6.9	14.4	45.9	20.0	29.5	26.0	11.3
N_2	7.6	13.6	46.0	23.4	29.5	36.0	9.2
O_2	6.8	12.2	19.4	22.2	14.3	18.7	8.6
CO_2	8.5	12.2	18.9	26.1	28.4	30.2	13.4
CH_4	9.6	13.6	20.7	27.6	27.6	48.9	27.1

PPO-powder, while the ratio were lowered in other membranes. It could be possible that CS_2 and TCE solvents did not change the conformation of the PPO molecules during membrane formation. Both solvents, i.e. CS_2 and TCE, have low boiling points in comparison to other solvents, which were used for the membrane preparation. Aromatic ring in the other solvents may have played an important role in such interaction. Yang and Li [41] reported the ESR spectra of polyaniline films of different thicknesses deposited on Pt and Au electrode. The thicker the film, the smaller the peak-to-peak line width, suggesting that the degree of delocalization is better for thicker films. Tsuji and Seiki [42] studied the ultraviolet irradiated PPO by ESR technique and observed the ESR signal intensity due to PPO radical was larger in the presence of air than under vacuum or in the presence of nitrogen. Similar behavior was also observed by Khulbe et al. [35] on unirradiated PPO-powder or in films prepared from it by using different solvents, i.e. carbon disulfide, benzene, 1,1,2 trichloroethylene (TCE), toluene, chlorobenzene and bromobenzene with few exceptions. The membranes were characterized simultaneously by atomic force microscope, ESR and RS. Permeation data for N_2, O_2, CO_2, and CH_4 were taken by using a constant volume gas permeation system.

Froyer et al. [43] prepared poly(phenylene) (PP) by using two different polymerization procedures. Although, the two products were very similar from a structural point of view, their magnetic properties as seen by ESR were very different. They interpreted this by correlating the number of spins with the number of structural defects that were probably formed during the polymerization process. Barbarin et al. [44] synthesized PP by various methods. Their ESR study suggested that: (i) the nature of paramagnetic centers is independent of annealing time and only spin concentration increases when the polymer is annealed for a longer time; (ii) a single kind of paramagnetic center is formed regardless of the annealing time; and (iii) no significant anisotropy of the *g* factor is detected.

Kaptan and Tatar [45] studied mechanical fracture of PMMA by ESR technique and reported that the ESR spectrum of PMMA depended on the vacuum conditions. They reported that oxygen converted the PMMA radicals into the peroxy radicals.

3.3. Spin-labeling method

A stable radical can also be introduced into polymeric material. The radical so introduced is often called a spin label or a spin probe. It is invariably nitroxide radical which exhibits a three-line hyperfine structure whose peak shape, splitting etc. depend on the radical's environments. The nitroxide label is a monitor of motion. The shape of the ESR signal depends also on the orientation of the magnetic field relative to the axis of the radical. Thus, the spin label method is useful to study the environment of radical, which is the structure of the polymer at a molecular level.

Table 3
Ratio of spins/g in different membranes in presence of different gases

Ratio of spins/g	PPO-powder	PPO–CS_2	PPO–C_6H_6	PPO–TCE	PPO–$CH_3C_6H_5$	PPO–ClC_6H_5	PPO–BrC_6H_5
CO_2/CH_4	0.894	0.897		0.945		0.617	0.494
O_2/N_2	0.985	0.897	0.421	0.948	0.484	0.519	0.941

The application of this method to the synthetic polymeric system is still in an infant stage. Probably, Stone [46] is the first who introduced the paramagnetic nitroxide radical into the polymer (synthetic polypeptides). Russian researchers have been foremost in the application of spin probes [47]. Tormala et al. [48,49] and Bullock et al. [50,51] tried to explore further the application of nitroxide radical in a study of synthetic polymers. Spin labeling in synthetic polymers has been discussed by Miller [52].

The main advantages of spin label ESR are: (i) the relative sensitivity of the technique; (ii) the comparative ease of measurements; and (iii) the versatility in the range of different spin labeling in synthetic polymers, as has been discussed by Miller [52]. A specific site of a molecule can also be labeled by choosing the appropriate spin label and reaction condition. Although a radical is introduced into polymeric material; in most cases, by removing the solvent from a solution of nitroxide and polymer, it has also been carried out by adsorption of nitroxide vapor into the polymer matrix and by direct dissolution of nitroxide into a molten polymer.

A potential problem involved in all aforementioned methods is the homogeneous distribution of nitroxide. However, the *g* and components (Hamiltonian parameters) of the radical do not vary greatly from one spin label to another. The spin-labeled molecule introduces some steric perturbation, but it is relatively small compared with the size of the polymer molecule. In comparison with nonperturbing techniques it is calculated that the size of this perturbation is tolerable at the label concentration normally used. The minimum working sample concentration depends on the width of the spin label spectra. In nonviscous solvents for small spin label nitroxide, a spin concentration of 5–10 μmol should be sufficient. For moderately immobilized spectra a concentration of 50 μmol is required and for strongly immobilized spectra a concentration of 30 μmol. It must be stressed that, for normal measurements on membrane samples, the spin label must be diluted to avoid the effects of dipole–dipole interaction (<1 mol% of the total lipid concentration in biological membranes) between spins.

Khulbe et al. [53] prepared dense homogeneous PPO membranes by casting a solution which consists of PPO, TEMPO (spin probe) and TCE solvent. The solvent was evaporated at 22, 4 and −10°C. Membranes were subjected to ESR spectroscopic study as well as to the permeability measurement of various gases, including O_2, N_2, CO_2 and CH_4. The permeability showed a minimum for each pure gas and the permeability ratio showed a maximum at 4°C for gas pairs of O_2/N_2 and CO_2/CH_4. The surface morphology of the membranes and the membrane selectivity depended on the temperature (22, 4 and −10°C) at which solvent was evaporated.

Veksli and Miller [54] studied the effect of good solvents on molecular motion of nitroxide free radicals covalently labeled to polystyrene and PMMA and observed that in all solvents the nitroxide radical was attached to a methacrylate unit through an amide linkage. In another study [55] they studied the effects of good solvents on the molecular motion of nitroxide free radical doped in the above polymers. It was found that the nitroxide radical was attached to a methacrylate unit through hydrogen bonding in the latter case. They have also concluded that the covalently bonded and doped radicals behaved qualitatively in a similar fashion. From the temperature dependence of ESR spectrum two types of spins in PMMA were found. Tormala et al. [48] and Tormala and Lindberg [49] observed that in nitroxide radical, introduced in solid polymers (polyamides and polyesters), the mobility of the end group radicals is severely restricted.

3.4. ESR application for fouling study

Oppenheim et al. [56] applied the ESR spectroscopy to the study of protein fouling in UF membrane. Their preliminary results showed that ESR was an ideal method for analyzing short time solute uptake in UF and indicated that the proteins on the membrane surface had a different conformation than the proteins trapped and lodged in the membrane pores. They suggested that the proteins within the pores might be more compressed than those on the surface. The ESR study of isotropic membranes can help to find the mechanism of mass transportation, mechanism of fouling in RO and UO membranes and other related fields.

3.5. Various other ESR studies on membranes

Paramagnetic ions may be used instead of nitroxide radicals as spin probes. Rex and Schlick [57] have used Cu^{2+} to study cross-linked polyacrylamide gel and found that the ESR (Cu^{2+}) line width was related to the pore size in the gel. The time dependent ESR spectra of Cu^{2+} found in crosslinked poly(vinyl alcohol) gels were simulated by Suryanarayana [58]. It was suggested that the segmental motion of the polymer chain could play a role in spin-probe motion. Similar types of study on RO membranes may provide better understanding for electrolyte transport through the membranes.

Bartl et al. [59] investigated the formation of two dimensional structure of polypyrrole films prepared by

electrochemical polymerization by ESR technique and reported that the line width of polypyrrole radical increased almost linearly with increasing oxygen pressure. The intensity of the ESR signal became more than 10 times when the oxygen pressure was atmospheric pressure as compared with that in vacuum. Successive repetitions of oxygen exposure/pump off procedures showed an excellent reversibility. Zhang and Lin [60] studied the oxygen permeability and O_2/N_2 permselectivity of a cobalt-neutralized sulfonated ionomer membrane by ESR technique. The membrane promoted the transport of molecular oxygen, which indicated that polymer complexes were formed in the ionomer. It could be possible that rapid and reversible binding of oxygen molecule is repeated through consecutive coordination sites when oxygen molecule is transported through the membrane. The O_2 binding was confirmed by ESR spectra. This work supported the suggestion that free radicals may take part in gas transport in the membrane [38]. Kim et al. [61] did ESR study on the segmental mobility and free volume decay of poly(phenyl methacrylate) films and calculated free volume.

ESR technique offers an investigator or a manufacturer several advantages over other methods of membrane characterization. The ESR provides information without disturbing the membrane. In future the ESR will help to find the fouling mechanism of the membranes and it will help to develop membranes of less fouling. The role of paramagnetic radicals in mass transport will also be studied by ESR technique. There has been some concern that in polymer matrices, measurements obtained through changes of ESR spectra with temperature may depend on the characteristics of the spin probes used. It was reported by Kusumoto [62] that the spectral narrowing temperature was shifted to higher values with larger probe.

4. Atomic force microscope

4.1. General principle

Binnig et al discovered that a flexible cantilever with a very low spring constant could be produced [63]. With a cantilever that induced forces smaller than inter-atomic forces, the topography of the sample could be measured without displacing the atom. The atomic force microscope creates topographic images of the surface by scanning a sample under a sharp stylus. The stylus is attached to a cantilever, which is deflected as a stylus interacts with the surface. The stylus may be in direct contact with the surface or it may be vibrated above the surface (noncontact). For high-resolution imaging and most routine topographic profiling, the systems are kept in direct contact with the surface. The noncontact method has been used to image magnetic and electronic fields, liquid films and soft surfaces (for example polymeric membranes).

Measuring the deflection of the cantilever as the sample is scanned under the stylus on x, y, and z directions piezoelectric translator produces images. The most common techniques for measuring the deflection are (i) measuring the phase of a laser light (an interferometer technique) and (ii) measuring the deflection of a laser beam that bounces off the back of the cantilever (the optical-lever technique). AFM was first applied to polymer membrane surface by Albrecht et al. in 1988 shortly after its invention [64]. AFM opened a new door for the study of membrane surfaces. AFM's noncontact mode is specially suited for the study of soft materials such as polymeric membranes. In this mode of operation, the tip is at some distance from the surface, generally 5–10 nm, and is responding to attractive van der Waals interactions with force of typically 10^{-12} N. This mode of operation is specially suitable for samples which are soft or liable to mechanical damage.

Digital Instruments (Santa Barbara, CA) patented TM AFM mode (Tapping Mode) which is widely used to study membranes (synthetic and biological). In this mode a fast oscillating probe is employed for surface imaging and a short, intermittent sample contact prevents the development of inelastic surface deformation. The vertical separation between the probe tip and the surface is rapidly oscillated such that probe taps the surface lightly. The discontinuous contact eliminates any lateral forces exerted on a surface by the scanning tip. However, the roughness parameters depend on the treatment of the captured surface data (plane fitting, flattening, filtering, etc.). Therefore, the roughness parameter obtained from AFM images should not be considered as absolute values.

4.2. Surface roughness

It is generally assumed that the surfaces of synthetic membranes, which are prepared from polymeric materials and used for various membrane separation processes, have to be smooth. It is often experienced however, in the process of the preparation of polymeric membranes, the membranes with patterns on the surface are obtained and regarded as undesirable. On the contrary, the surfaces of biological membranes are characterized by some patterns. It is easy to understand why patterned surfaces are more advantageous for the material transport to biological systems when an increase in the surface area available in a limited space is considered. There could be other hidden advantages due to pattern on the surfaces. It would, therefore, be advantageous for a synthetic polymeric membrane to possess a pattern so that a larger area effective for the material transport can be incorporated in a limited space of an industrial module. It is reported that the mean roughness of the membrane (measured by AFM) was directly proportional to the permeability of gases (Fig. 12) with exception of PPO–TCE membrane. The roughness parameter for PPO–TCE membrane was very low in comparison with other studied membranes (Fig. 12). Gould et al. [65] studied the surface of poly(ethylene terephthalate) (PET) films by AFM

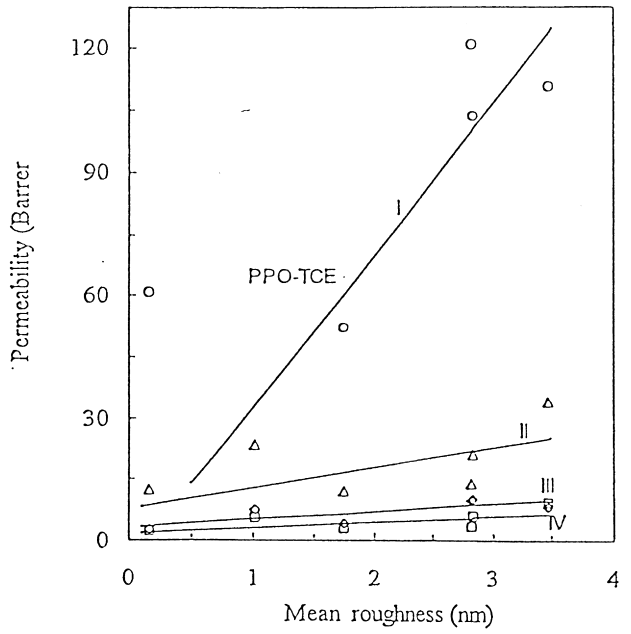

Fig. 12. Permeability (Barrer) of gases vs. mean roughness (nm) of membrane (top surface); I-○: CO_2; II-△ O_2; III-diam;: CH_4; IV-□: N_2.

and reported that the surface roughness can distinguish between the amorphous and crystalline regions. They also suggested that irregularities on the surface could affect the film's physicochemical properties of the film.

Membrane fouling is the primary impediment to a wide use of RO and UF in water treatment processes. Colloidal particles are the major culprits for the fouling of the RO membranes. However there are other factors such as sparingly soluble salts, dissolved organic solvents, microorganisms etc. [66]. During colloidal fouling of RO membranes, colloidal particles accumulate at the membrane surface and increase the resistance to water flow through the membrane. Colloids are ubiquitous in natural and process water. Examples include clays, colloidal silica, oxylhydroxide, large organic macromolecules, organic colloids, suspended matters and precipitated calcium carbonate.

The fundamental mechanism controlling the fouling of the RO membranes is complex and not well understood. Elimelech et al. [67] studied the surface morphology by AFM in colloidal fouling of cellulose acetate and composite aromatic polyamide RO membranes. They observed higher fouling rate for the thin film composite membrane compared to that for the cellulose acetate membrane. The higher fouling rate for the thin film composite membrane was attributed to surface roughness, which was inherent in interfacially polymerized aromatic polyamide composite membranes. The surface images revealed that the thin film composite membrane exhibited large-scale surface roughness of ridge-and-valley structure (Fig. 13), while the cellulose acetate membrane surface was relatively smooth (Fig. 14). Hirose et al. [68] found a relationship between the flux of RO membranes and their roughness parameters determined by AFM. According to their experiments, an increase in surface roughness resulted in a higher water permeation flux.

4.3. Membrane pore size

Bessieres et al. [69] reported that the size of pores measured by AFM for sulfonated polysulfone (SPS) UF membranes could be used to predict the separation data of polyethylene glycol. Thus, the morphology of the surface may take an important part in the transportation of materials. Bowen et al. [70] used noncontact AFM to investigate the surface pore structure of Cyclopore and Anopore MF membranes in air. Analysis of the image gave quantitative information on the surface pore structure, in particular the pore size distribution. To understand the role of surface, AFM technique is a very effective tool. This study will give a new direction for the desirable membrane formation for the industrial use.

Dietz et al. [71] reported the AFM images of three capillary pore MF membranes and eight UF membranes. Fritzche et al. presented AFM images of poly(vinylidene fluoride) MF membranes [72], polyethersulfone UF membranes [73,74] and poly(acrylonitrile) [75] UF membranes. These results were discussed by Nakao [2] and it was reported that the characteristics of membranes were reasonable regarding pore size and pore size distribution of the membrane. Bessieres et al. [69] used AFM to investigate the surface of polymeric UF and MF membranes. In their work, surface pore structure and distribution of pore size on the polyethersulfone membrane were studied. Their microscopic techniques had discerned pore diameters in the range of 11–114 nm for 40–200 kDa molecular weight cut-off (MWCO) SPS UF membranes and confirmed a mean pore diameter of 96 nm for the 0.1 μm polyvinylidenefluoride (PVDF) MF membrane. Fig. 15 shows topography of a 40 kDa SPS membrane observed in air by AFM. They suggested that AFM could provide information on the structure and shape of pore apertures.

The school of Bowen [70,76] used noncontact AFM to investigate the pore structure of a polyethersulfone UF membrane (polyethersulfone of specific MWCO of 25 000 (E625, PCI membrane system)). Excellent images were obtained at single pore resolution. They successfully compared their data with the previously reported data obtained by other methods and recommended that AFM was a very informative technique for the study of UF membranes. In another study they measured the pore size of six commercial membranes by AFM using noncontact mode [70,76]. The results are given in Table 4, which shows an excellent agreement between the pore sizes measured by AFM and those quoted by the supplier. Recently they developed a new technique for measurement of adhesion force of a single particle by using AFM. This method could be useful for the development of new membrane materials with low or zero fouling property [70].

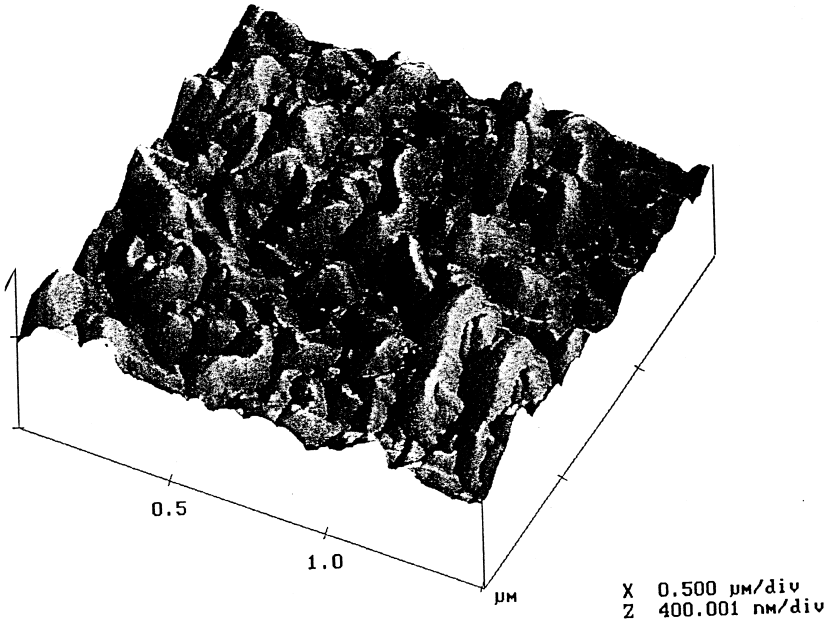

Fig. 13. AFM image of the composite RO membrane. The *Z*-axis scale is 400 nm per division and the *X*-axis scale is 500 nm per division.

Recently, Singh et al. [77] characterized various UF and nanofiltration membranes by solute transport and by AFM. Mean pore sizes measured by AFM were about 3.5 times larger than calculated from the solute transport. Moreover, pore sizes measured by AFM were remarkably fitted to the long-normal probability distribution curve.

4.4. Nodules on the membrane surface

Hamza et al. [78] prepared thin film composite nanofiltration membranes by coating a thin layer of sulfonated polyphenylene oxide (ion exchange capacity = 1.93 meq/g dry polymer) on top of a porous polyethersulfone substrate membrane. The coating solutions were prepared by dissolving 1 wt.% of SPPO polymer in chloroform/methanol mixtures of different compositions. It was noted that the intrinsic viscosity decreased with an increase in chloroform in the solvent mixture, indicating that the polymer molecule coiled more compactly in a solvent mixture with higher chloroform content. The surface investigation of the membranes by AFM revealed their nodule like structure. The nodule size decreased also with an increase in chloroform

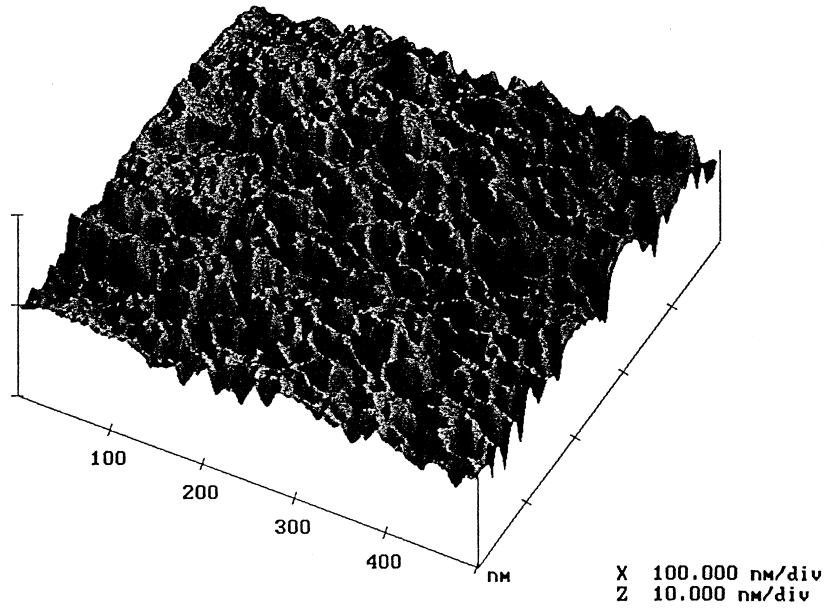

Fig. 14. AFM image of the cellulose acetate RO membrane. The *Z*-axis scale is 10 nm per division and the *X*-axis scale is 100 nm per division.

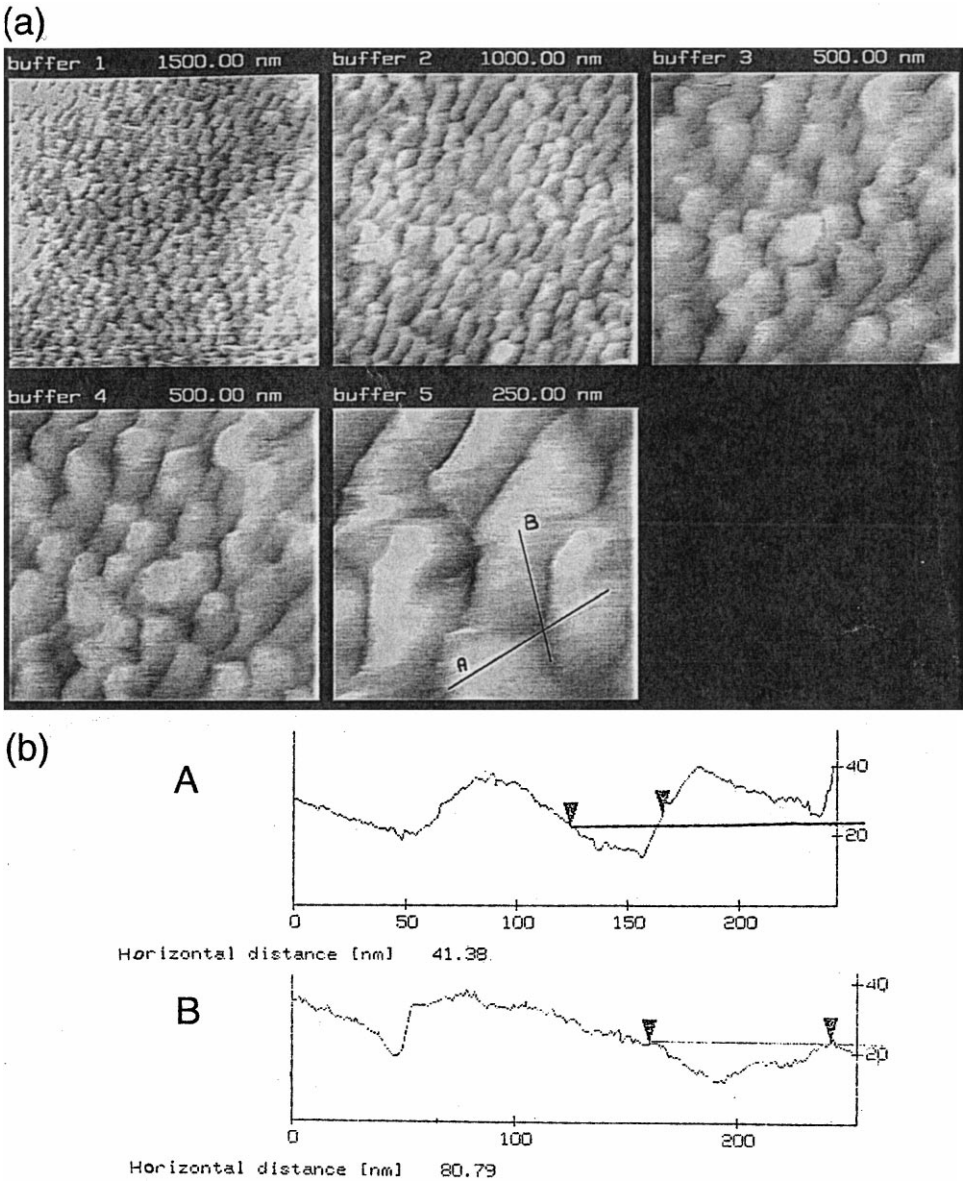

Fig. 15. (a) Topography of a 40 kDA SPS membrane observed in air by AFM (several scanned areas), (b) line profiles of the last precedent image. One pore is evidenced by the markers. The horizontal distance between each pair is reported below. These measurements give pore diameters of $d_p = 41$ nm and $D_p = 81$ nm, respectively.

content in the solvent mixture. This means that compactness of the polymeric coil in the coating solution is retained after evaporation of the solvent from the solution. The effect of the chloroform concentration in the solvent mixture on the membrane flux was dramatic. In the separation experiment of sodium chloride solute, the flux decreased from 11 to less than 2×10^{-6} m^3/m^2s as the chloroform concentration increased from 0 to 66%. It indicates that the nodule size plays a role in the performance of the membrane.

Surface morphology of asymmetric and homogeneous membranes prepared from PPO using trichlorethylene (TCE) as a solvent was studied by tapping mode AFM [79]. Membranes were prepared by spreading the casting solution on a glass plate and the solvent was removed by evaporation at room temperature. As expected, a significant difference in the morphology between the top and bottom surface was observed. The observed difference in morphology between the top and bottom surfaces of homogeneous membrane was rather unexpected. Figs. 16 and 17 show the representative 3D image of the bottom and top surfaces of the homogeneous membrane, respectively. It can be noticed that both surfaces show a relatively uniform nodular structure; however, nodules of the bottom surface ($d = 137.5$ nm) are twice as large as those on the top surface ($d = 63.8$ nm). The mean roughness of the bottom and top surfaces was 0.757 and 0.376 nm, respectively.

Dense (homogeneous) membranes were prepared from PPO by using TCE as a solvent at different solvent evaporation

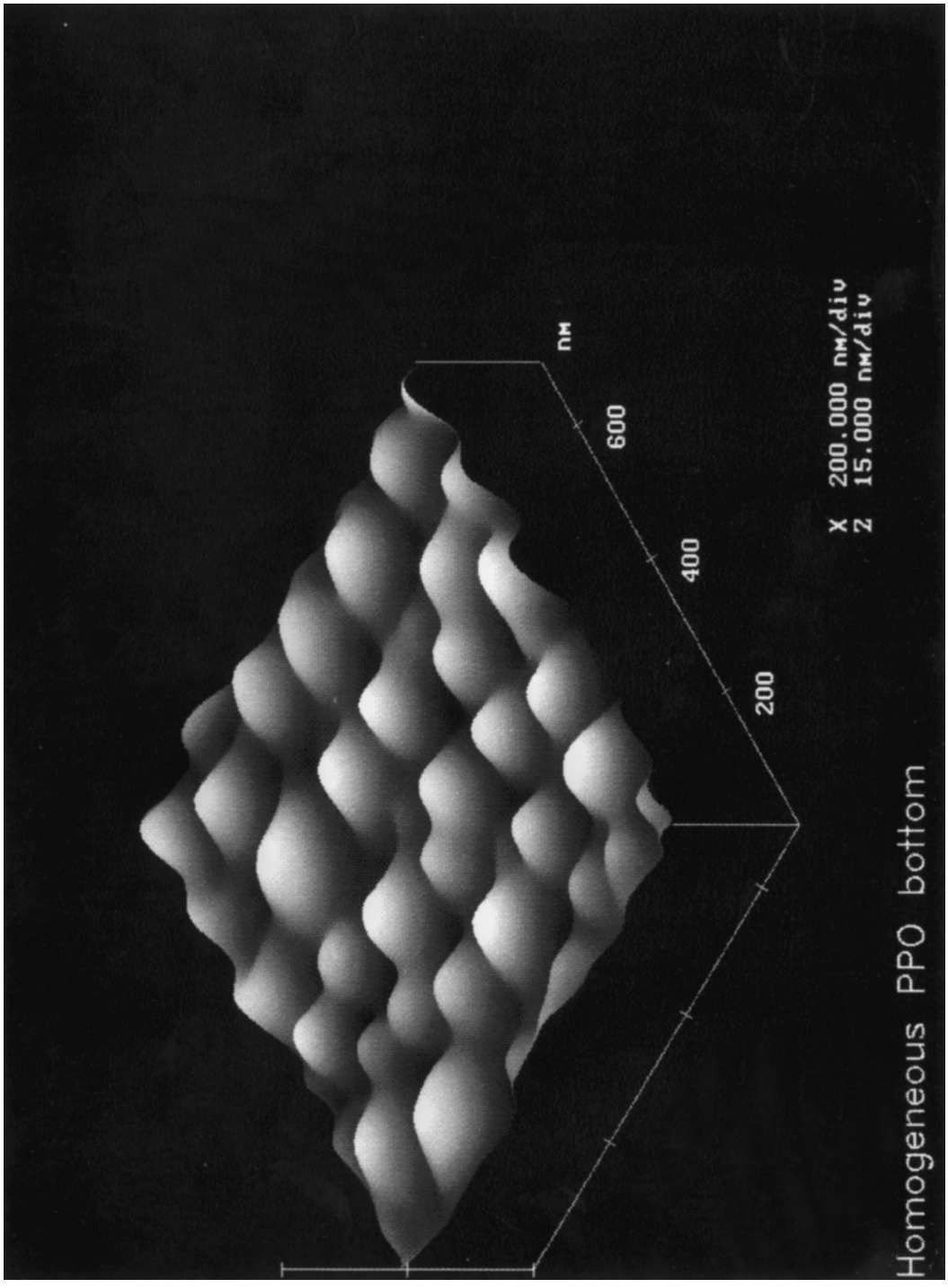

Fig. 16. Surface plot of the image by TM AFM of the homogeneous membrane's bottom surface.

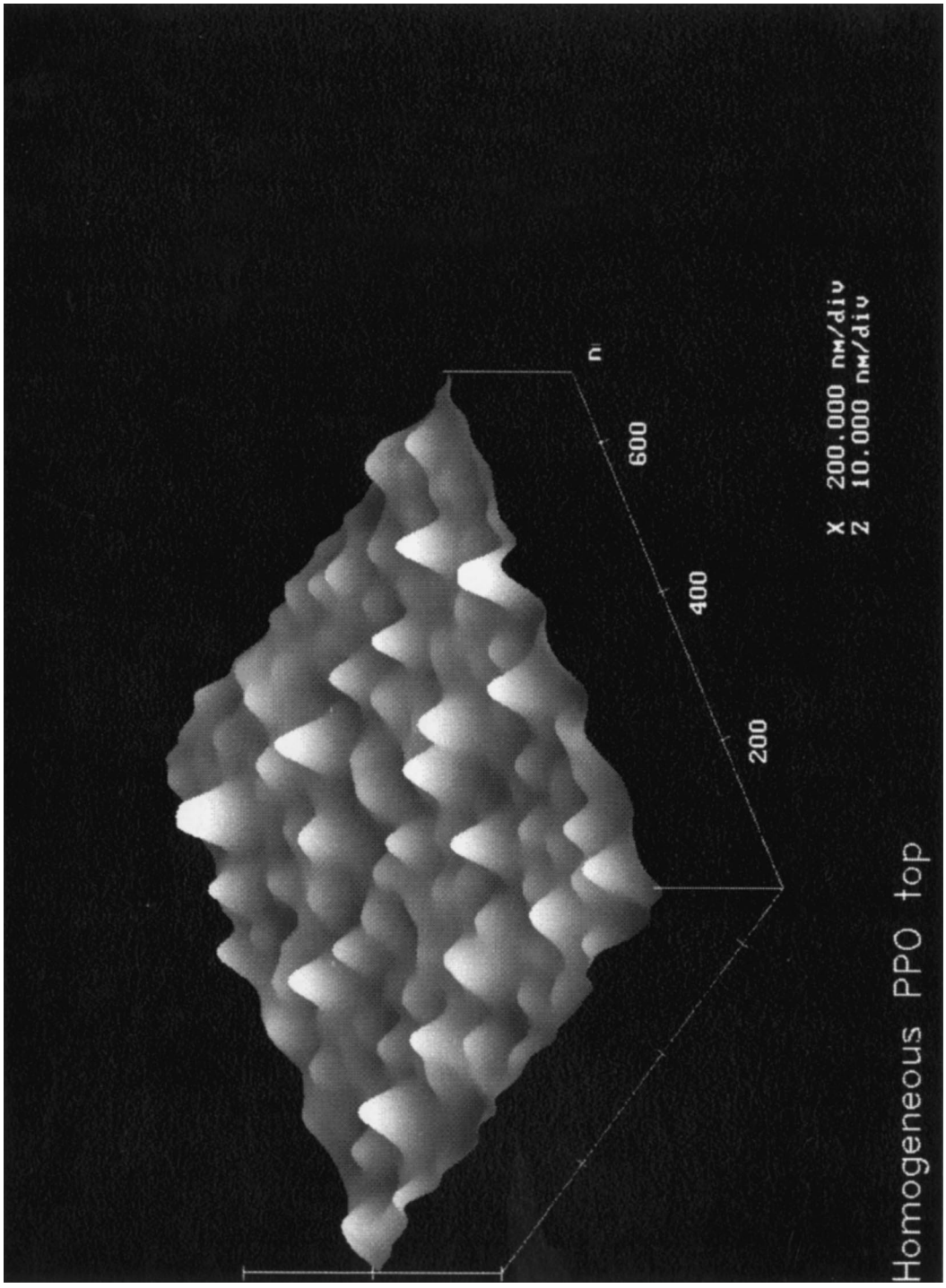

Fig. 17. Surface plot of the image by TM AFM of the homogeneous membrane's top surface.

Table 4
Pore size of Cyclopore and Anopore membranes quoted by the supplier and measured by AFM

Cyclopore membranes[a]		Anopore membranes[a]	
Nominal pore size[b] (μm)	Measured by AFM (μm)	Nominal pore size[b] (μm)	Measured by AFM (μm)
0.1	0.109	0.02	0.0279
0.2	0.184	0.1	0.108
0.4	0.412	0.2	0.188

[a] Whatmann International Ltd.
[b] Quoted by supplier.

temperatures (22, 4 and −10°C). It was observed that the morphology of the surface on the membrane depended on the temperature used for the preparation of the membranes. It was also observed that the selectivity of CO_2/CH_4 and N_2/O_2 in the studied membranes depended on the temperature. Khulbe et al. [53] suggested that if a membrane consisting of a *single nodule size* of higher molecular ordering could be prepared, the membrane selectivity would increase with a decrease in casting temperature.

Lehman et al. [80] studied the surface of Nafion 117 membrane by TP AFM and observed supermolecular structure of membrane, which was made of nodules of a mean diameter of 11 nm. The nodules were surrounded by interstitial regions of a mean thickness of 50 Å. They tried to co-relate swelling properties of the membrane with its surface morphology. Khulbe et al. [81] studied the effect of thickness of PPO films on the surface morphology by AFM technique and tried to co-relate the mean size of nodules and the roughness parameters with Marangoni and Releigh numbers.

4.5. Miscellaneous (general morphology)

Kolonits [82] reported that, for cellulose acetate film formed using ethyl acetate as solvent, a honeycomb structure resulted on its surface. On the contrary, chloroform produced a fine granular structure. Katz and Munk [83] reported the influence of the solvent or substrate on the water vapor permeability of films. They reported that the polarity of the solvent had a definite influence on the permeability of the film. Thus, the morphology of the surface may take an important part in the material transport. Recently, a great deal of attention has been given to the morphology of the membrane surfaces and an attempt has been made to correlate the surface characteristics with the performance of the membrane [35]. Kasper et al. [84] investigated the samples of Cuprophan (Trade Name) flat sheet membranes as well as samples of modified membranes containing 5, 10, 15, 20, 40 and 100% diethylamino ethyl cellulose (DEAE). They demonstrated the AFM ability to show characteristic difference in the surface morphology of different cellulose based membranes in a state where preparation artifacts can be excluded.

Zhiqlang et al. [85] studied the surface morphology of composite ceramic membranes which were made of $Al_2O_3-SiO_2-TiO_2$ by AFM, with the aid of X-ray analysis. Four different types of phases were identified; i.e. crystalline $Al_4Ti_2SiO_{12}$ ($2Al_2O_3-SiO_2-2TiO_2$), Al_2O_3, TiO_2 and noncrystalline SiO_2. No binary oxides were detected. They reported that surface morphologies of the composite membrane were significantly affected by compositions. Existence of TiO_2 phase resulted in a smooth surface; on the other hand SiO_2 resulted in a rougher phase. However, they did not give any data of the surface morphology effect on the practical use. Prater et al. [86] improved the scanning ion conductance microscope by using micro fabricated probes. These new probes imaged the surface topography of a plastic diffraction grating, and the ion flow through porous polycarbonate membrane filters.

AFM is an effective means of investigating the surface structure of membranes. The surface topography of membranes can be explored without distortion of the membrane surface. The AFM should be considered as the method of the first choice for determination of the surface pore and distribution of pores in MF membrane. In future, AFM of very high resolution will be fabricated where we will be able to determine pore sizes in gas separation membranes in angstrom units and it will help us solve the controversial theory for gas transport.

Accumulated knowledge of tip sample force interactions has led to better understanding of AFM for polymer surface. In the early stage of AFM discovery, the question was posed by the 1987 paper, ‘The Atomic Force Microscope’. Can it be used to study Biological Molecules? [87]. It was answered by Hansama and Noh [88] as ‘yes’. Similarly, we may be able to answer ‘yes’ to the question; ‘Will AFM be applicable for the measurement of pore sizes in the gas separation and RO membranes in the future?’

5. Other methods

Amiji and Park [89] examined the adsorption of poly(ethylene oxide)/poly(propylene oxide) (PEO/PPO/PEO) triblock polymers (Pluormics) on dimethyldichloride treated glass (DDS0) by radiolabeling and fluorescence techniques. Iversen et al. [90] characterized the microporous membranes for use in membrane contactors by the mass

transfer mechanism of SO_2 through gas filter pores. They tried to correlate the experimentally determined mass transfer coefficient to intrinsic physical properties of the membrane by applying theoretical and empirical correlations for the porosity–tortuosity relationship of the porous structure, thereby limiting fluxes could be predicted with good accuracy from data quoted in the manufacturer's catalogue.

Recently, Kulkarni et al. [91,92] studied the pore structure in cellulose acetate UF and RO membranes by using small angle neutron scattering technique. Experiments were carried out on dry membranes as well as on membranes swollen with deuterated solvents (D_2O and CD_3OD) and it was reported that the pore structure in UF membranes was smooth and nonfractal in nature. The estimated pore sizes obtained for dry, D_2O swollen and CD_3OD swollen UF membranes agreed well with pore sizes determined by electron microscopy. In ultrathin cellulose acetate membranes, they reported the presence of very small (10–20 Å) porous structure. Davis and Smith [93] analyzed the pore structure of coating on paper by NMR and observed that there was good agreement between the data obtained by NMR and the conventional method, i.e. mercury porometery. The main advantage in the NMR method is that it does not require dry samples and can study pore sizes over a broad range.

6. Conclusions

It is concluded that Raman spectroscopy, ESR and AFM are powerful tools to characterize polymeric membranes. The special features of each method can be summarized as follows.

RS is effective to investigate:

1. Inter and intramolecular interactions working among macromolecules through their functional groups.
2. Crystalline structure of the macromolecules in the membrane.
3. Change of polymer structure during membrane formationt
4. Thermal effect on polymeric structure in the membrane.
5. Interfacial study of lamelar or coated membrane.

ESR is effective to investigate:

1. Degree of molecular ordering in the assemblage of polymer chains.
2. Mobility of macromolecules and permeate molecules in the membrane.
3. Interaction between the radical size in the membrane and the permeate.
4. Mobility of electrolyte radical such as Cu^{2+} in the polymeric membrane..
5. Mechanism of membrane fouling.
6. Mechanism of thin layers coating.

AFM is effective to investigate:

1. Pore size and pore size distribution of membranes.
2. Surface roughness.
3. Size of macromolar nodules.
4. Change of the surface during the fouling.
5. Interaction forces working between the permeate and the membrane surface.

References

[1] Loeb S, Sourirajan S. Adv Chem Ser 1962;38:117.
[2] Nakao S. J Membrane Sci 1994;96:131.
[3] Galeski A, Pirkowska E. J Polym Sci, Polym Phys Ed 1983;21:1313.
[4] Glotin M, Domszy R, Mandelkern L. J Polym Sci 1983;21:285.
[5] Alamo R, Domszy R, Mandelkern L. J Phys Chem 1984;88:6587.
[6] Dybal J, Stokr J, Schneider B. Polymer 1983;24:971.
[7] Koenig JL. Appl Spectrosc Rev 1971;4:233.
[8] Tashiro K, Takano K, Kobayashi M, Chatani Y, Tadokoro H. Polymer 1983;24:199.
[9] Rabolt JF. CRC Crit Rev Solid State Mater Sci (USA) 1984;12:165.
[10] Ko H, T HJ. Appl Polym Sci 1996:59.
[11] Ohnishi T, Murase I, Noguchi T, Hirooka N. Synth Met 1986;14:207.
[12] Koenig JL, Angood CA. J Polym Sci, Polym Phys 1970;8:1787.
[13] Boerio FJ, Koenig JL. J Polym Sci, Polym Symp 1973;43:205.
[14] Gall MJ, Hendra PJ, Peacock CJ, Cudby MEA, Willis HA. Spectrochim Acta Part A 1972;28:1985.
[15] Zerbi G. Adv Infrared Raman Spectrosc 1984;11:301.
[16] Grasselli JG, Snavely MK, Marcia K, Bulkin BJ. Phys Rev 1980;65:231.
[17] Lu CS, Koenig JL. Ame Chem Soc Div Org Coatings Plast Chem 1972;32:112.
[18] Koenig JL, Shih PTK. J Polym Sci, Polym Phys Part A-2 1972;10:721.
[19] Evans RA, Hallam HE. Polymer 1976;17:838.
[20] Gailliez-Degremont E, Bacquet M, Laureyns J, Morcellet M. J Appl Polym Sci 1997;65:871.
[21] Gillberg G. J Adhesion 1987;21:129.
[22] Delhaye M, LeClereq M, Landon DC. Ind Res 1977;19:69.
[23] Adar F, Noether H. In: Gooley R, editor. Microbeam analysis, San Francisco: San Francisco Press, 1983. pp. 269.
[24] Dhamelincourt P, Wallart F, Leclereq M, Nguyen AT. Anal Chem 1979;51:414A–7A 420A–421A.
[25] Swalen JD, Scholtter NE, Santo R, Rabolt JF. J Adhes 1981;13:189.
[26] Miller DR, Han OH, Bohn PW. Appl Spectrosc 1987;41:249.
[27] Scholtter CE, Rabolt JF. Appl Spectrosc 1984;38:208.
[28] Gall MJ, Hendra P. The spex Speaker 1971;16(1):1.
[29] Gall MJ, Hendra PJ, Peacock CJ, Cudby MEA, Willis HA. Polymer 1972;13:104.
[30] Zubov I, Voronkov VA. Vysokomol Soedin, Ser B 1968;10:92 ca. 68 (1968) 36306g.
[31] Frazer GV, Hendra PJ, Cudby ME, Willis HA. J Mater Sci 1974;9:1270.
[32] Schlotter NE, Rabolt JF. J Phys Chem 1984;88:2062.
[33] Rabolt JF, Swalen JD. Adv Spectrosc 1988;16:1 Chickester, UK.
[34] Willis HA. In: West A, editor. Molecular spectroscopy, New York: Heyden, 1977.
[35] Khulbe KC, Matsuura T, Lamarche G, Kim HJ. J Membrane Sci 1997;135:211.
[36] Khulbe KC, Kruczek B, Chowdhury G, Gagne S, Matsuura T, Verma SPJ. Membrane Sci 1996;111:57.
[37] Carrington A. Endeavour 1962;21:51.
[38] Khulbe KC, Chowdhury G, Matsuura T, Lamarche G. J Membrane Sci 1997;123:9.
[39] Unpublished data.
[40] Al'tschuler SA, Kozyrev BM. In: Poole Jr. CP, editor. Electron paramagnetic resonance, New York: Academic Press, 1964. pp. 312–3.
[41] Yang SM, Li CP. Synth Met 1993;55–57:636.

[42] Tsuji K, Seiki T. Polym J 1973;4:589.
[43] Froyer G, Maurice F, Bernier P, Andrew P. Polymer 1982;23:1103.
[44] Barbarin F, Berthet G, Blanc JP, Fabre C, Germain JP, Hamdi M, Robert H. Synth Met 1983;6:53.
[45] Kaptan HY, Tatar L. Appl Polym Sci 1997;65:1161.
[46] Stone TJ, Buckman T, Nordio PL, McConnell HM. Proc Natl Acad Sci USA 1965;54:1010.
[47] Buchachenko AL, Kovarskii AL, Wasserman AM. In: Rogovin ZA, editor. Study of polymers by the paramagnetic method: advances in polymer science, New York: Halsted Press, 1976. pp. 255–72.
[48] Tormala P, Silvennoinen K, Lindberg JJ. Acta Chemica Scandinavica 1971;25:2665.
49 Tormala P, Lindberg JJ. Spin labels and probes in dynamic and structural studies of synthetic and modified polymers. In: Ivin KJ, editor. Structural studies of macromolecules by spectroscopic methods, New York: Wiley, 1974. pp. 255–72.
[50] Bullock AT, Cameron GG, Smith PM. Macromolecules 1976;9:650.
[51] Bullock AT, Cameron GG, Krajewski V. J Phys Chem 1976;80:1790.
[52] Miller WG. Spin labeled synthetic polymers. Molecular biology spin labeling II: theory and application. New York: Academic Press, 1976, pp.173–302.
[53] Khulbe KC, Chowdhury G, Kruczek B, Vujosevic R, Matsuura T, Lamarche GJ. Membrane Sci 1997;126:115.
[54] Veksli Z, Miller WG. Macromolecules 1977;10:686.
[55] Veksli Z, Miller WG. Macromolecules 1977;10:1245.
[56] Oppenheim SF, Buettner GR, Dordick JS, Rogers VGJ. J Membrane Sci 1994;96:289.
[57] Rex GC, Schlick S. Polymer 1987;28:2134.
[58] Suryanarayana D. J Appl Phys 1988;63:4110.
[59] Bartl A, Dunsch L, Naarmann H, SchmeiBer D, Gopel W. Synth Met 1993;61:167.
60 Zhang Z, Lin S. Gaofenzi Xuebaco 1997;1:55 ca. 126, 200 153.
[61] Kim SS, Yavrouian AH, Liang RH. J Polym Sci, Part B, Polym Phys 1993;31:495.
[62] Kusumoto N. Kagaku no Ryoiki 1979;33:380 ca. 91, 141 357n.
[63] Binnig G, Quate C, Gerber Ch. F. Phys Rev Lett 1986;56:930.
[64] Albrecht TR, Dovek MM, Lang CA, Grutter P, Quate CF, Kuan SNJ, Frank CW, Pease RFW. J Appl Phys 1988;64:1178.
[65] Gould SAC, Schiraldi DA, Occelli ML. J Appl Polym Sci 1997;65:1237.
[66] Cohen RD, Probstein RF. J Colloid Interface Sci 1986;114:194.
[67] Elimelech M, Zhu X, Childress AE, Hong S. J Membrane Sci 1997;127:101.
[68] Hirose M, Itoh H, Minamizaki Y, Kamiyama Y. Proceedings of the International Congress on Membranes and Membrane Process. Yokohama, Japan, 18–23 August 1996, pp. 178–179.
[69] Bessieres A, Meireles M, Coratger R, Beauvillain J, Sancbez V. J Membrane Sci 1996;109:271.
[70] Bowen WR, Hilal N, Lovitt RW, Williams PM. J Membrane Sci 1996;110:233.
[71] Dietz P, Hansama P, Inacher KO, Lehmann HD, Herrmann K-H. J Membrane Sci 1992;71:101.
[72] Fritzsche AK, Arevalo AR, Moore DM, Elings VB, Kjoller K, Wu CM. J Membrane Sci 1992;68:65.
[73] Fritzsche AK, Arevalo AR, Connolly AF, Moore MD, Elings VB, Wu CM. J Appl Polym Sci 1992;45:1945.
[74] Fritzsche AK, Arevalo AR, Moore MD, Weber CJ, Elings VB, Kjoller K, Wu CM. J Appl Polym Sci 1992;46:167.
[75] Fritzsche AK, Arevalo AR, Moore MD, O'Hara. J Membrane Sci 1993;81:109.
[76] Bowen WR, Hilal N, Lovitt RW, Williams PM. J Membrane Sci 1996;110:229.
[77] Singh S, Khulbe KC, Matsuura T. J Membrane Sci 1998;142:111.
[78] Hamza A, Chowdhury G, Matsuura T, Sourirajan S. J Membrane Sci 1997;129:55.
[79] Khulbe KC, Kruczek B, Chowdhury G, Gagne S, Matsuura T. J Appl Polym Sci 1996;59:1151.
[80] Lehmani A, Durand-Vidal S, Turq P. J Appl Polym Sci 1998;68:503.
[81] Khulbe KC, Matsuura T, Noh H. J Membrane Sci 1998;145:243.
[82] Kolonits V, Kolloid ZZ. Polymer 1968;226:40.
[83] Katz R, Munk BF. J Oil Color Chem Ass 1969;52:418.
[84] Kasper K, Herrmann KH, Dietz P, Hansma PK, Inacker O, Lehmann H-D, Rintelen Th. Ultramicroscopy 1992;42:1181.
[85] Zhiq1ang Z, Xiaoyue X, Zhilun G, Longtu L. J Membrane Sci 1997;136:153.
[86] Prater CB, Hansma PK, Tortonesse M, Quate CF. Rev Sci Instrum 1991;62:2634.
[87] Person BN. J Chem Phys Lett 1987;141:366.
[88] Hansma HG, Noh JH. Annu Rev Biophys Biomol Struct 1994;23:115.
[89] Amiji MM, Park K. J Appl Polym Sci 1994;52:539.
[90] Iversen SB, Bhatia VK, Dam-Johansen K, Jonsson G. J Membrane Sci 1997;130:205.
[91] Kulkarni S, Krause S, Wignall GD. Macromolecules 1994;27:6785.
[92] Kulkarni S, Krause S, Wignall GD, Hammouda B. Macromolecules 1994;27:6777.
[93] Davis PJ, Smith DM. TAPPI J 1989;May:85.